Revista de Chimie
https://revistadechimie.ro
https://doi.org/10.37358/Rev.Chim.1949

Study on Degradation of Lignin by TiO_2-based Photocatalyst Doped with Carbon Dots

YU TAN, MINGYU HE, YING LI, MAMATJAN YIMIT*
Xinjiang University, College of Chemical Engineering, Key Laboratory of Oil and Gas Fine Chemicals, Ministry of Education and Xinjiang Uyghur Autonomous Region, 666 Shengli Road, Tianshan District, Urumqi City, Xinjiang Province, China

Abstract: *The carbon dots were prepared by the microwave method, and then the TiO_2 doped with carbon dots was successfully synthesized by the hydrothermal method. Its structure was investigated using TEM, XRD and XPS. The catalyst was applied to the degradation of lignin base solution (50 mg of lignin in 30 mL of sodium hydroxide solution pH = 12) under ultraviolet light. It was found that when the mass ratio of carbon point to TiO_2 was 1.5:1, the dosage of catalyst was 0.75 g/L, and the degradation time was 6 h, the degradation rate could reach more than 45%. The degradation rate of more than 40% could be maintained after seven cycles, indicating that the catalyst had good photocatalytic cycle stability. The degradation products were analyzed by GC-MS, and the main products were n-butyl acetate, butyl phthalate and alkanes with long carbon chains.*

Keywords: *carbon dots, lignin photocatalysis, TiO_2 catalyst, ultraviolet light*

1.Introduction

Lignin is the only natural polymer material with aromatic structure in nature, which is composed of sinapyl alcohol group, coniferyl alcohol group and p-coumary alcohol group connected by 4-O-5, α-O-4, β-O-4, β-β, β-1, 5-5 and other bonds. Its typical structure is shown in Figure 1 [1-3]. However, the complex chemical structure of lignin makes it impossible to be used directly, it usually needs to be degraded before it is used. The lignin can be degraded to obtain products such as low molecular weight phenols and organic acids [4, 5]. These degradation products are not only important chemical raw materials but also can be converted into liquid fuels through hydrogenation and deoxygenation reactions.

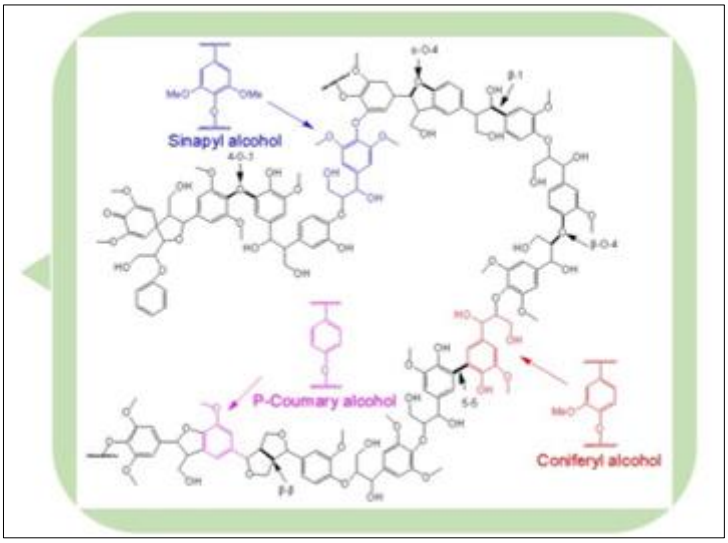

Figure 1. Structure diagram of lignin

There are many degradation methods of lignin, such as enzymolysis, pyrolysis, hydrolysis and oxidative degradation. However, these methods all have some disadvantages, for example, enzymatic

**email: mmtj10@sina.com*

hydrolysis reaction conditions for temperature, pressure requirements, difficulty to industrialization; Reunion of degradation products occurs; The degradation rate is not high and so on [6]. Photocatalysis has been considered as the optimal degradation method due to its advantages of cleanness, high efficiency and low cost [7].

Gu et al. [8] used the La-modified SBA-15/H_2O_2 system as a catalyst to desorb lignin at the microwave power of 200 W and 150°C. After 10 min, monophenols with a mass yield of 2.7% were obtained. Wang et al. [9] prepared carbon-modified nickel catalyst by carbothermal reduction method, and studied the catalytic oxidation and hydrolysis of lignin sulfonate with it. The results showed that the three-dimensional electron distribution of nickel was changed by carbon modification, and it had a high selectivity for the hydrolysis of C-O bonds of lignin to generate aromatic hydrocarbons, with a yield of up to 22%.

At present, the most widely used photocatalyst is TiO_2, which has the advantages of non-toxicity, stable chemical properties and low price [10, 11]. However, due to the low utilization of visible light and the electron-hole recombination [12-14], it is often necessary to modify it. The commonly used modification methods include ion doping, surface deposition of precious metals, surface photo-sensitization and so on [15-19].

It has been reported that carbon dots (CDs) can promote the photocatalytic activity of the materials [20]. It can convert longwave band light into short wave band light, to broaden the light absorption band of the material, and CDs also has a large electron storage capacity, which helps the transfer of photogenerated electrons in the material and inhibits the composite of electrons and holes [21-23]. Therefore, in theory, modification of TiO_2 with CDs can effectively improve the two shortcomings of TiO_2 as a photocatalyst.

Yiqing Deng et al. [24] used CDs/TiO_2 to degrade methyl orange and found that the degradation rate could reach 70.56% under the irradiation of 600 nm light source. The results of fluorescence spectrum analysis and UV-Vis showed that the CDs could convert 600 nm visible light to 350 nm ultraviolet light. Zhang Bo et al. [25] used hydrothermal method to combine CDs and TiO_2, and investigated the degradation effect of composite catalyst on pulping black liquor under visible light. The results showed that most of the organic matter in the pulping black liquor was degraded, and the COD_{Cr} removal rate was 81.2%.

Under the irradiation of ultraviolet light, the alkali-lignin was degraded to obtain n-butyl acetate, butyl phthalate and alkanes with longer carbon chains.

2. Materials and methods

2.1. Raw materials and instruments

Lignin, homemade [26], extracted from waste cotton stalks collected in the southern Xinjiang region of Xinjiang Uygur Autonomous Region, china; Nano TiO_2 (particle size =100 nm, anatase, hydrophilic); Ethylenediamine (> 99.0%); Anhydrous ethanol (> 99.0%); Citric acid (analytically pure); Photo-chemical reactor, homemade (internal UV lamp is 1000 W, 300~400 nm); Microwave Reactor (700 W); Dialysis bag (MD44-1000); Ultrasonic cleaner (KQ-100VDB type); Hydrothermal reactor (containing 100 mL PTFE lining); Blast drying oven; Centrifuge.

2.2. The preparation of CDs/TiO_2

The citric acid (1 g) was added into distilled water (10 mL) and stirred until completely dissolved. Ethylenediamine (500 mg) was added to it and stirred for 10 min. Then the mixed solution was placed in a microwave reactor and reacted for 5-7 min until a red-brown solid was generated. Once it has cooled to room temperature, distilled water (30 mL) was added to it and stirred until completely dissolved. In a centrifuge, it was centrifuged for 20 min at 3000 r/min. Then, 2/3 of the supernatant liquid was poured into a dialysis bag, and dialyze for 3 days. After dialysis, the solution was concentrated by a rotary evaporator and dried to obtain reddish-brown powder CDs.

A (125,250,375,500) mg CDs was added into a beaker containing anhydrous ethanol solution (20 mL), afterward, distilled water (40 mL) was added into it, and ultrasonic dispersion was carried out at room temperature for 1 h. After ultrasonic dispersion, 250 mg TiO_2 was added to the mixture and then ultrasonic dispersion was carried out for 1 h to obtain a uniformly dispersed mixture. The mixed solution was transferred to a hydrothermal reaction autoclave for reaction at 120ºC for 5 h. After the reaction was completed, the kettle was allowed to cool naturally to room temperature, the mixed solution was taken out, centrifuged at 3000 r/min for 20 min, and collected the precipitate. Then the precipitate was washed three times with distilled water and dried at 60℃ for 12 h to obtain CDs/TiO_2 doped with a mass ratio of 0.5:1,1.0:1,1.5:1,2.0:1.

2.3. Characterization of CDs/TiO_2

TEM: TiO_2 and CDs/TiO_2 were uniformly dispersed in ethanol solution and dropped on copper mesh. After drying, the surface morphology of TiO_2 and CDs/TiO_2 was observed by high-resolution transmission electron microscope (JEOL-JEM-2100F).

XRD: Cu-Ka (λ=0.154056 nm) was used to study the structure of TiO_2 and CDs /TiO_2 at 2θ=5° ~ 80° by powder X-ray diffraction (Ultima IV) technique. Then, the grain diameter perpendicular to the (hkl) crystal plane was calculated by Debye - Scherrer's equation:

$$D_{hkl} = \frac{K\lambda}{\beta_{hkl}\cos\theta} \quad (1)$$

D_{hkl} is the grain diameter perpendicular to the (hkl) crystal plane, K is the Scherrer constant, λ is the incident wavelength, β is the half peak width (rad) of the diffraction peak, θ is the Bragg's diffraction Angle. Finally, the lattice parameters of tetragonal titanium dioxide (hkl) crystal plane can be calculated by the following formula

$$\frac{1}{d^2} = \frac{h^2+k^2}{a^2} + \frac{l^2}{c^2} \quad (2)$$

d is the spacing of crystal faces, a and c are lattice parameters

XPS: X-ray photoelectron spectroscopy (Thermo scientific K-Alpha) was used to analyze the surface chemical information of CDs/TiO_2.

UV-vis DRS: The absorption range of CDs/TiO_2 was measured by ultraviolet/visible diffuse reflectance test (PE lambda 750), with $BaSO_4$ as reference, and the test wavelength was 200～800 nm. Then the band gap width of the material can be calculated from Kubelka-Munk equation:

$$(\alpha h\nu)^n = B(h\nu - E_g) \quad (3)$$

α is the absorbance (absorbance); h is Planck's constant; ν is the frequency of light; B is a constant related to material; E_g is the band gap energy value; indirect band gap semiconductor n=1/2, direct band gap semiconductor n=2.

BET: According to N_2 adsorption-desorption isotherm at 77K, it was calculated by multi-point Brunauer-Emmett-Teller (BET: Mike-tristar ii3flex) method. The BET surface area was measured in a relative pressure range from 0.05 to 0.3. The average porosity is calculated by quenched density functional theory (QSDFT).

TGA: The thermal stability was analyzed on a thermogravimetric analyzer (TGA5500). It is tested in nitrogen at a heating rate of 10ºC /min from room temperature to 800ºC.

GC-MS: The product was dissolved in ethyl acetate and its components were analyzed by GC-MS (QP2010-SE).

2.4. Degradation of lignin by CDs/TiO_2 under ultraviolet light

Lignin (50 mg) was dissolved in NaOH solution (30 mL) with *p*H=12 and added a certain amount of CDs/TiO_2 to it. Then the mixture was placed on a magnetic stirrer and reacted for some time at room temperature under the irradiation of a 1000 W UV lamp. At the end of the reaction, the solid and liquid were separated at a speed of 3000 r/min in the centrifuge, and the solid was CDs/TiO_2. The liquid was extracted with ethyl acetate (15 mL). After extraction, the oil phase of the extract was analyzed by GC-MS and the aqueous phase was acidified to *p*H=3, then dried and weighed in a blast furnace. The degradation rate is calculated as the following formula:

$$\eta\ (\%) = [(m_{all} - m_{residual})/m_{all}] \times 100\% \quad (4)$$

η is degradation rate, m_{all} is Initial quality of lignin, $m_{residual}$ is quality of residual lignin.

CDs/TiO_2 obtained by centrifugation was vacuum freeze-dried and recycled. The recovered CDs/TiO_2 was used as catalyst again in the degradation reaction of lignin. The degradation rate was calculated, and the lifetime of lignin was evaluated by the change value of degradation rate.

The effects of three factors were investigated including the doping mass ratio of CDs and TiO_2, the addition amount of catalyst, and the degradation time. Besides, considering the economic effect of the catalyst, we also experimented on the reutilization of the catalyst.

3. Result and discussions

3.1. Degradation results

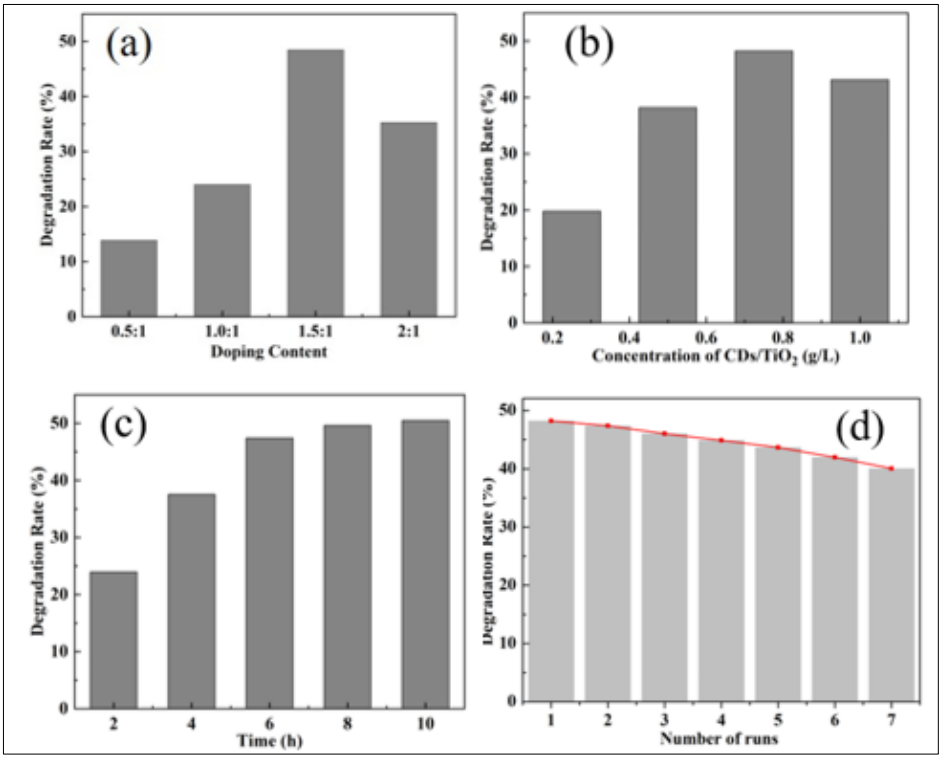

Figure 2. (a) influence of doping amount of CDs on degradation rate (reaction condition: degradation time of 6 h, CDs/TiO_2 concentration of 0.75 g/L) (b) influence of CDs/TiO_2 concentration on degradation rate (reaction condition is the degradation time of 6 h, the doping mass ratio of CDs and TiO_2 is 1.5:10) (c) effect of reaction time on degradation rate (the reaction condition is that the doping mass ratio of CDs and TiO_2 is 1.5:10, and the CDs /TiO_2 concentration is 0.75 g/L) (d) CDs/TiO_2 recoverability test (reaction conditions: the doping mass ratio of CDs and TiO_2 is 1.5:10, CDs /TiO_2 concentration is 0.75 g/L, and the reaction time is 6 h)

According to Figure 2a, when the doping mass ratio of CDs and TiO_2 is 1.5:1, the degradation rate reaches the maximum of 48.45%. When the doping mass ratio of CDs to TiO_2 is less than 1.5:1, the degradation rate increases with the increase of the number of CDs. This is because within this range, the addition of CDs is beneficial to reduce the electron-hole recombination generated by TiO_2 itself, and at the same time, the band gap energy becomes low, which is conducive to the degradation reaction. When the doping mass ratio of CDs to TiO_2 is greater than 1.5:1, the degradation rate begins to decrease with the increase of the number of CDs. This is because the excessive addition of CDs accumulates on the surface and channels of TiO_2 and hinders light collection, so the degradation rate becomes low at the same degradation time.

According to Figure 2b, when the concentration of CDs/TiO_2 is 0.75 g/L, the degradation rate reaches a maximum of 48.23%. When the concentration of CDs /TiO_2 is less than 0.75 g/L, the degradation rate increases with the increase of the concentration of CDs/TiO_2. This is because the increase of CDs/TiO_2 amount represents the increase of active site of catalyst, which can produce more effective photons, which is conducive to the degradation reaction [27]. When the concentration of CDs/TiO_2 is greater than 0.75 g/L, the degradation rate begins to decrease with the increase of the concentration of CDs/TiO_2. This is because the concentration of the CDs/TiO_2 is equal to 0.75 g/L, per unit time of effective photon has reached saturation in solution, more CDs/TiO_2 is unable to produce a more effective photon. In addition, excessive CDs/TiO_2 will cause light scattering and cover each other, so that the generation rate of effective photons decreases. Therefore, the degradation rate becomes lower in the same degradation time [28].

According to Figure 2c, the degradation rate increases with the increase of reaction time. This is because the longer the reaction time is, the longer the illumination time is, the more light-energy TiO_2 gets, the more electron-hole pairs are generated, and the higher the degradation rate of lignin. However, after the reaction time reached 6 h, the increase in degradation rate was not significant (47.39% at 6 h, 49.61% at 8 h and 50.47% at 8 h). This is because the reaction time is too long, and the small molecules generated by degradation undergo micro-polymerization. On the whole, the optimal reaction time is 6 h and the degradation rate is 47.93%.

According to Figure 2d, the degradation rate decreases with the increase of the number of cycles. However, CDs/TiO_2 can still maintain a degradation rate of more than 40% after being used 7 times, which indicates that CDs/TiO_2 has good stability and can be recycled.

3.2.TEM of CDs /TiO_2

To observe the surface morphology of CDs/TiO_2, the TEM was performed. Figure 3 shows TEM images of TiO_2 and CDs/TiO_2. Through comparing the two figures, we can see that there are many small white spots on the surface of CDs/TiO_2. In addition, we did not find free CDs, indicating that CDs and TiO_2 are closely combined [29]. From Figure 3a and Figure 3b, it can be seen that the dispersion of nano-TiO_2 itself is not good, so the dispersion of CDs/TiO_2 is not good, and the agglomeration phenomenon appears. Moreover, CDs/TiO_2 is formed by the precipitation of CDs on the surface of TiO_2. From Figure 3c, we can see the characteristic lattice fringes of TiO_2 in the complex, and the spacing between crystal faces is 0.339 nm, which corresponds to the characteristic crystal faces (101) of anatase type TiO_2, indicating that the nanometer titanium dioxide we used is anatase type.

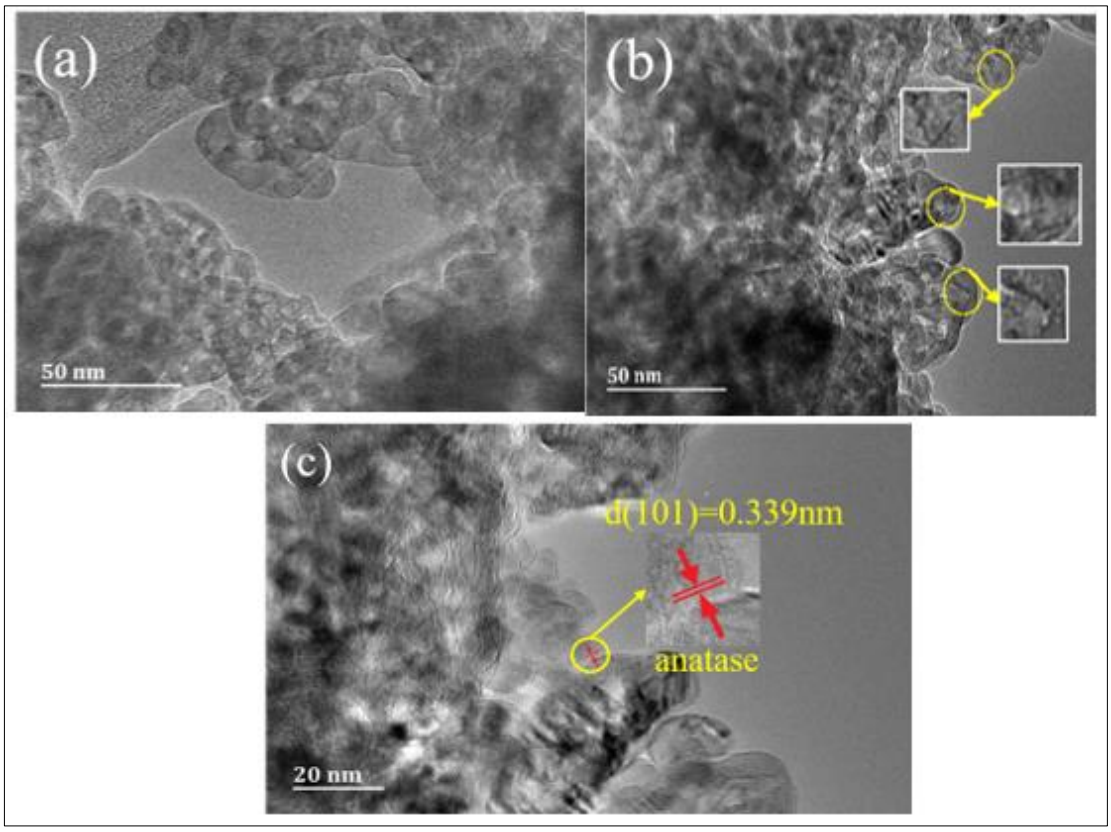

Figure 3. TEM images of (a) TiO_2 (b) CDs/TiO_2 (c) Typical lattice Fringe of Anatase Phase TiO_2

3.3. XRD of CDs/TiO_2

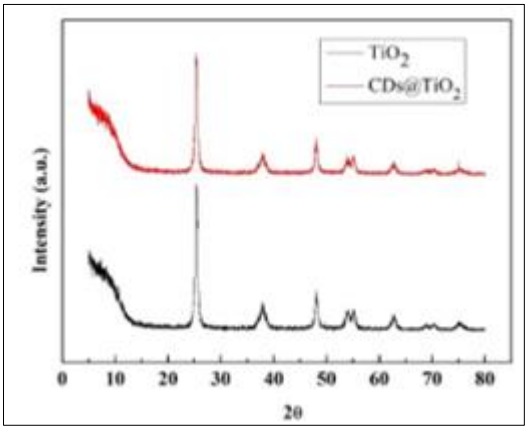

Figure 4. XRD patterns of TiO_2 and CDs/TiO_2

To understand the crystal structure of CDs/TiO_2, the XRD was done. Figure 4 shows the XRD patterns of TiO_2 and CDs/TiO_2. Firstly, the analysis of TiO_2 shows that the material has obvious diffraction peaks at $2\theta = 25.2°$, 37.7°, 47.8°, 53.6°, 54.8° and 62.5°, which correspond to (101), (004), (200), (105) and (211) crystal planes. This is the same as the crystal plane parameters of anatase TiO_2 [30], indicating that the purchased TiO_2 is anatase TiO_2. In addition, the diffraction peak in XRD is sharp and strong, which indicates that CDs/TiO_2 is single crystal structure and has good crystallinity.

According to the XRD analysis of CDs/TiO_2, we can see that both the diffraction peak position and the intensity of the diffraction peak correspond well with the spectrogram of TiO_2, which shows that TiO_2 has good stability and that doping CDs into TiO_2 has no effect on the crystal form and crystal structure of TiO_2, and TiO_2 in the synthesized CDs/TiO_2 completely retains its original structure.

According to eq.1, the grain diameter of anatase TiO_2 used by us along the direction perpendicular to the (101) crystal plane is 21.831 nm.

As can be seen from Figure 3c, the interplanar spacing of the titanium dioxide (101) crystal plane in the complex is d = 0.339 nm, and h = 1, k = 0, l = 1 of (101) crystal plane. According to eq. 2, we can calculate a = 3.7781 Å, c = 9.4737 Å. The deviation between the lattice constant of TiO_2 and the tetragonal anatase cell (a = 3.7821 Å, c = 9.5022 Å) may be related to the doping of CDs.

3.4. XPS of CDs/TiO_2

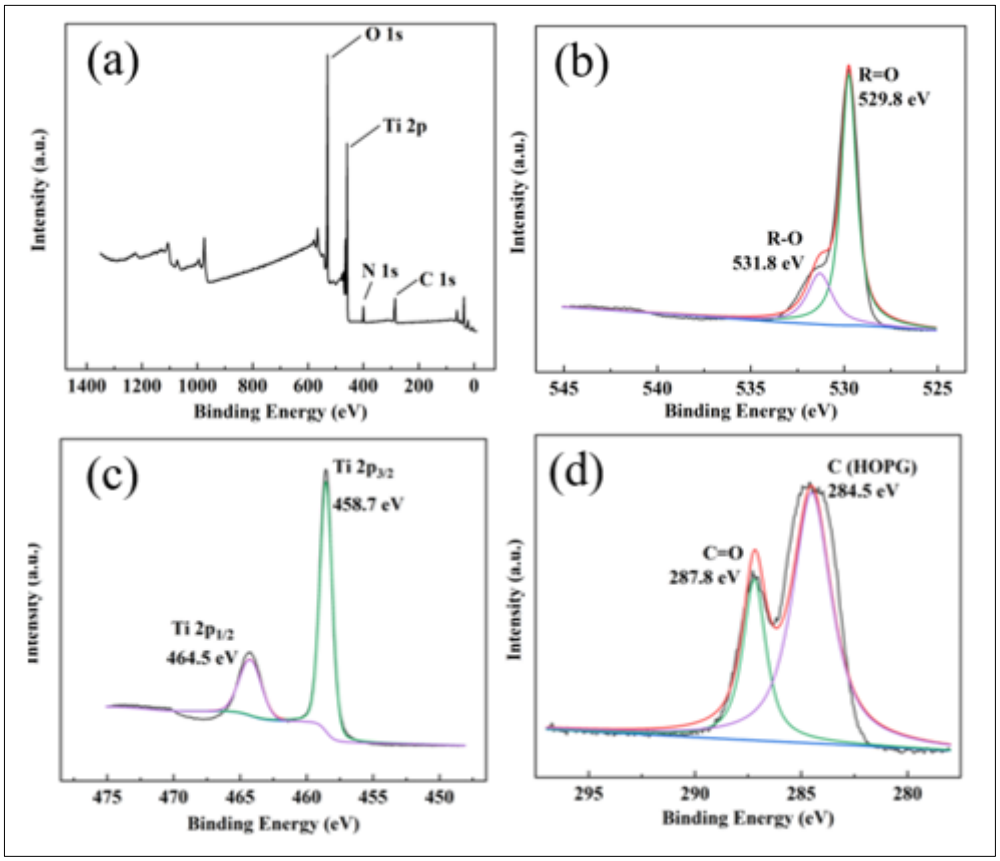

Figure 5. XPS diagram of CDs/TiO_2 (a) Survey (b) O 1s (c) Ti 2p (d) C 1s

To understand the chemical element information on the surface of CDs/TiO_2, the XPS was performed. Figure 5 shows the XPS spectra of CDs/TiO_2. In the full spectrum of Figure 5a CDs/TiO_2, we can see the absorption peaks of O1s, Ti2p, N1s and C1s, this indicates that the composite material is composed of O, Ti, N and C elements (the appearance of N element is due to the presence of ethylene-diamine in the raw materials used to prepare CDs). And the proportion between them is Ti 2p =20.86%, O 1s=49.5%, C 1s=23.65%, N 1s=5.98%. In Figure 5b O 1s spectra, we can see the absorption peaks at 529.8 eV and 531.8 eV, corresponding to R=O and R-O-R bonds respectively. The appearance of these two bonds is related to TiO_2 and CDs. In Figure 5c Ti 2p spectrum, we can see that there are absorption peaks at 458.7 eV and 464.5 eV, which correspond to Ti $2p_{3/2}$ and Ti $2p_{1/2}$ respectively. This indicates that the valence state of Ti in CDs/TiO_2 is Ti^{4+} [31]. In Figure 5d C 1s spectrogram, we can see that absorption peaks appear at 284.5 eV and 278.8 eV, corresponding to C-R and C=O bonds respectively. This is the same as the bond of CDs reported in the literature [32].

Through the above XPS analysis, we can confirm that CDs has successfully compounded on the surface of TiO_2, and Ti-O-C bond is formed between the two, which makes the two bond closely, which is corresponding to the analysis in TEM.

Moreover, the electron binding energy of Ti in CDs/TiO_2 indicates that TiO_2 is high-purity anatase type TiO_2, which is corresponding to the analysis in XRD.

3.5. UV-DRS of CDs/TiO_2

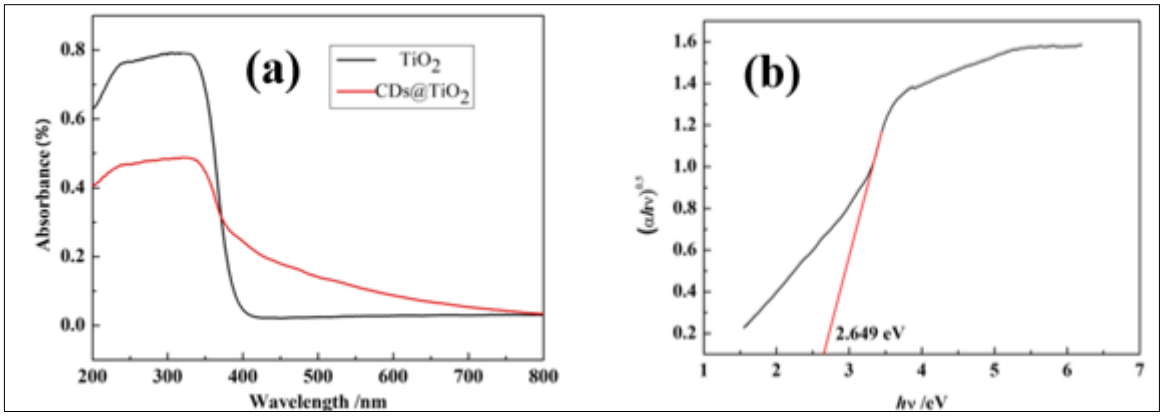

Figure 6. (a) UV-DRS diagram of TiO_2 and CDs/TiO_2 (b) The band gap width diagram of CDs/TiO_2 fitted by Kubelka-Munk equation

To study the optical properties of CDs/TiO_2, the UV-Vis DRS was performed. Figure 6 shows the UV-DRS diagram of TiO_2 and CDs/TiO_2 and the band gap width diagram of CDs/TiO_2 fitted by the Kubelka-Munk equation. According to Figure 6a, the absorption range of anatase TiO_2 is mainly concentrated in the ultraviolet region, while the absorption range of TiO_2 doped with CDs is from the ultraviolet region to the visible region, but it is mainly concentrated in the ultraviolet region. This shows that the absorption range of CDs/TiO_2 prepared by us has been expanded, which is attributed to the interaction of Ti-O-C bond between CDs and TiO_2 [33]. This interaction can effectively change the interface transmission rate of the carrier, which is beneficial to the catalytic action of TiO_2 in the visible light range.

According to the literature, for the anatase phase of TiO_2, being an indirect band gap semiconductor, the value of n is 0.5, and E_g is 3.20 eV [20]. From Figure 6b, we can find that the band gap energy of CDs/TiO_2 is 2.649 eV, and the CDs/TiO_2'sband gap energy is reduced by 0.551 eV. This shows that CDs/TiO_2 has better photocatalytic performance than ordinary TiO_2 [34]. As mentioned above, CDs can improve the catalytic effect of the catalyst by absorbing two or more photons with longer wavelengths, converting low-energy photons to high-energy photons. Therefore, we can speculate that CDs can act as electron mediators, photosensitizers and spectral converters in the process of photocatalysis.

3.6. BET of CDs/TiO_2

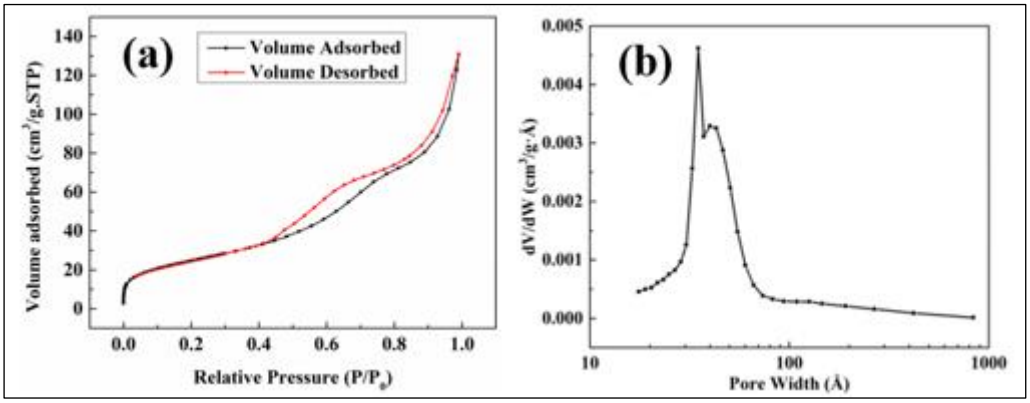

Figure 7. (a) N_2 adsorption and desorption curve of CDs/TiO_2 (b) pore size distribution of CDs/TiO_2

To study the pore structure of CDs/TiO_2, the BET was done. The specific surface area of solid catalysts plays an important role in the catalytic performance of photocatalysts. Catalysts with large specific surface areas have better photocatalytic performance because they provide a large number of

active sites and can effectively adsorb reactants. The specific surface area, pore size and pore volume of CDs/TiO_2 were studied by BET method. Figure 7 shows the N_2 adsorption and desorption curve of CDs/TiO_2 and the pore size distribution of CDs/TiO_2. According to the BET test, the specific surface area of CDs/TiO_2 is 89.2411 m^2/g, the average pore diameter is 72.059 Å, and the pore volume is 0.1915 cm^3/g. According to Figure 7a, the adsorption isotherm of CDs/TiO_2 follows the type IV isotherm of mesoporous nanomaterials. In addition, it can be seen that there is an H3 type hysteresis loop in the adsorption and desorption curve, which is mainly since the composite material is a mesoporous structure, and the capillary condensation phenomenon occurred during the test. It can be seen from the hysteresis loop of the H3 type that the hole in the composite material is wedge-shaped structure and does not show adsorption saturation in the region of high relative pressure. and according to Figure 7b, the pore size distribution is 34.9 Å. The larger specific surface area of CDs/TiO_2 ensures that lignin molecules can be fully adsorbed, which is conducive to the photodegradation of lignin molecules. Moreover, the narrower pore size distribution enables the composites to have more active sites.

3.7.Thermal gravimetric analysis of CDs/TiO_2

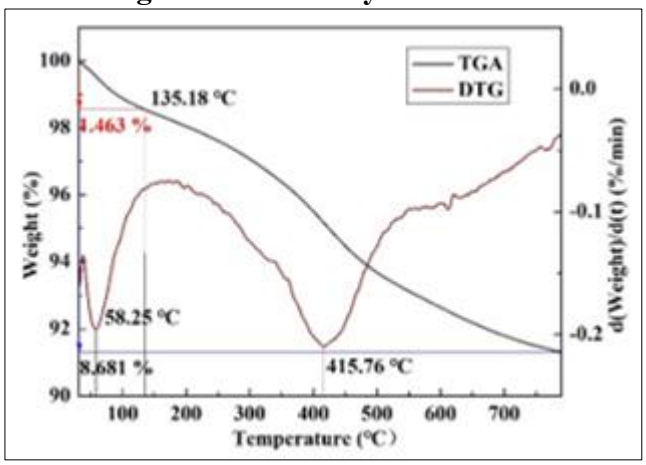

Figure 8. TGA and DTG curves of CDs/TiO_2

To study the thermal properties of CDs/TiO_2, the TG was done. Figure 8 shows the TGA and DTG curves of CDs/TiO_2 from room temperature to 790ºC in N_2 atmosphere. It can be found that the decline of the curve can be divided into two stages. The first stage is from room temperature to 135.18℃, and the second stage is from 135.18ºC to 790ºC. In the first stage, because the catalyst was not dried thoroughly, water was adsorbed on the surface and heated water was evaporated, the mass loss in this stage was 1.463%, and the fastest water loss temperature was 58.25ºC. The second stage corresponds to the decomposition of CDs/TiO_2, and the initial decomposition temperature of CDs/TiO_2 is 135.18ºC. The weight loss at this stage is mainly related to the bond breaking of oxygen-containing groups (such as epoxy group, carbonyl group, carboxyl group, etc.) on the surface of CDs and TiO_2 by covalent bonds [34], and the fastest decomposition temperature is 415.76ºC. In the whole thermal analysis process, the mass loss of CDs/TiO_2 is 8.681%, indicating that it has a higher thermal stability property.

3.8.The degradation mechanism

When the light irradiates TiO_2, the electrons in the valence band of TiO_2 will be excited and transition to the conduction band. However, TiO_2 has a wide band gap (3.20 eV), and the excited electrons tend to return to the valence band and recombine with the holes generated when excited. When CDs modified TiO_2, the band gap decreased to 2.649 eV, and the excited electrons were more likely to reach the conduction band, and the electrons would migrate to CDs.

The O_2 attached to the surface of the catalyst will react with the excited electron on the CDs to get the superoxide radical. H_2O reacts with the superoxide radical to get the hydroxyl radical. At the same time, the holes in the valence band of TiO_2 will convert water into hydroxyl radical. The hydroxyl radical can degrade lignin [35].

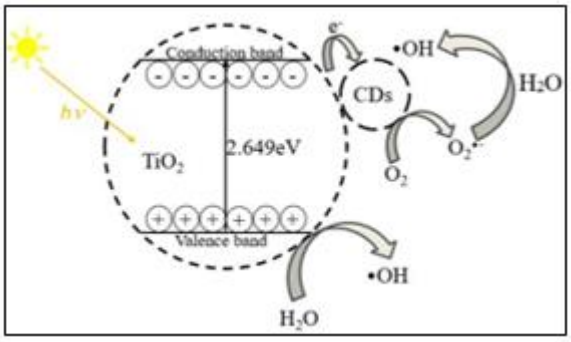

Figure 9. Charge separation and transfer diagram in CDs/TiO_2

Compared with TiO_2, CDs/TiO_2, due to the existence of CDs, the band gap energy becomes narrower, which means that the responsiveness to visible light is enhanced, more excited electrons can reach the conduction band, and more holes exist above the valence band so that the oxidation capacity is stronger [0].

Based on GC-MS analysis, we know that the products are n-butyl acetate, butyl phthalate and longer carbon chain alkanes (5,6-dimethyl-undecane and 2,6,10-trimethyl-dodecane). As can be seen from Figure 1, lignin does not have such a long carbon chain in its molecular structure, so there is no doubt that benzene ring opening and C-C bond breaking occurred in the degradation process. The presence of butyl phthalate indicates the presence of phthalic acid in the reaction, which may be due to the oxidation of the methoxy groups of the two side chains of the methoxy group to formic groups, the breaking of the remaining bonds, and then the reaction with the ring opening of the benzene ring and the breaking of the C-C bond to the butanol.

The presence of butyl acetate indicates the presence of acetic acid in the reaction, which may be derived from the cleavage of α-O-4 and β-O-4 and the oxidation of the alcohol derived from the cleavage of the C-C bond attached to the benzene ring, followed by reaction with butanol derived from the ring opening of the benzene ring and the cleavage of the C-C bond.

4.Conclusions

CDs was prepared by microwave method and then doped onto TiO_2 by simple hydrothermal synthesis. The surface morphology of CDs/TiO_2 was observed by TEM, and the results show that CDs has been successfully compounded to the surface of TiO_2. The crystal structure of CDs/TiO_2 was investigated by XRD, and the results showed that the addition of CDs did not affect the crystal form of TiO_2, and both TEM and XRD indicated that the TiO_2 used was anatase type TiO_2. XPS proves that the composite contains three elements, Ti, C and O, which proves that the catalyst is successfully synthesized, and the Ti-O-C bond is formed between CDs and TiO_2.

It was found by UV-Vis DRS technology that the edge of the absorption region of CDs/TiO_2 moved to the visible light region compared with that of pure TiO_2. Then, the band gap width of CDs/TiO_2 was calculated by the Kubelka-Munk equation, and it was found that the band gap width of CDs/TiO_2 decreased from 3.20 eV of pure TiO_2 to 2.649 eV. This indicates that CDs /TiO_2 has better photocatalytic performance. BET test shows that the adsorption isotherm of CDs/TiO_2 is IV isotherm, and its specific surface area is 89.2411m^2/g, with many active sites. In TGA, it can be seen that the weight loss curve of CDs/TiO_2 is divided into two sections. The first section is room temperature to 135.18^{o}C, with a weight loss rate of 1.463% and the fastest weight loss temperature of 58.25^{o}C. The second section is 135.18^{o}C to 790^{o}C, with a weight loss rate of 7.218% and the fastest weight loss temperature of 415.76℃. In the whole process, the weight loss rate of CDs/TiO_2 is 8.681%, which indicates that it has good thermal stability. The prepared CDs/TiO_2 catalyzed the degradation of lignin alkali solution under ultraviolet light, and the degradation rate reached more than 45%. The degradation products were mainly n-butyl acetate, butyl phthalate and alkanes with long carbon chains (5, 6-dimethyl-undecane, 2,6, 10-trimethyl-dodecane). All these indicate that lignin is expected to be degraded to produce raw materials for

traditional petrochemical products. In the end, a reasonable explanation of the mechanism of CDs/TiO_2 photocatalysis is proposed.

Acknowledgements: This work was funded by the National Natural Science Foundation of China (No. 21764013) and the Postgraduate Research Innovation Project of Xinjiang Uygur Autonomous Region (XJ2020G033 and XJ2021G032).

References

1.ZAKZESKI J., BRUIJNINCX P C. A., JONGERIUS A. L., et al. The catalytic valorization of lignin for the production of renewable chemicals, *Chemical Reviews*, **110**(6), 2013, 3552-3599.
2.PANDEY M. P., KIM C. S., Lignin Depolymerization and Conversion. A Review of Thermochemical Methods, *Chemical Engineering & Technology*, **34**(1), 2011, 29-41.
3.GUO F., SHI W., SUN W., et al. Differences in the adsorption of enzymes onto lignin from diverse types of lignocellulosic biomass and the underlying mechanism, *Biotechnology for Biofuels*, **7**(1),2014, 38.
4.BONINI C., MAURIZIO D., AURIA., MAGGIO P. D., et al. Characterization and degradation of lignin from steam explosion of pine and corn stalk of lignin: The role of superoxide ion and ozone, *Industrial Crops & Products*, **27**(2), 2008, 182-188.
5.XU L. C., Hydrolytic degradation of alkaline lignin in hot-compressed water and ethanol, *Bioresource Technology*, **101**(23), 2010,9308-9313.
6.SHU RIYANG, XU YING, ZHANG QI, et al. Progress in catalytic depolymerization of lignin, *CIESC Journal*, **67**(11) 2016, 4523-4532.
7.LI H, LEI Z, LIU C., et al. Photocatalytic degradation of lignin on synthesized Ag-AgCl/ZnO nanorods under solar light and preliminary trials for methane fermentation, *Bioresource Technology*, **175C**, 2015, 494-501.
8.GU X., KANGHUA C., MING H., et al. La-modified SBA-15/H_2O_2 systems for the microwave assisted oxidation of organosolv beech wood lignin, *Maderas-Cienc Tecnol*, **14**(1), 2012, 31-41.
9.MIN W., ZHANG X, LI H., et al. Carbon Modification of Nickel Catalyst for Depolymerization of Oxidized Lignin to Aromatics. *Acs Catalysis*, **8**(2), 2018, 1614-1620.
10.PELAEZ M., NOLAN N. T., PILLAI S. C., et al. A Review on the Visible Light Active Titanium Dioxide Photocatalysts for Environmental Applications. *Applied Catalysis B Environmental*, **125** 2012, 331-349.
11.CHENBO WANG, ZIFEI JIANG, LIN WEI, et al. Photosensitization of TiO_2 nanorods with CdS quantum dots for photovoltaic applications: A wet-chemical approach, *Nano Energy*, **1**(3), 2012, 440-447.
12.YU J., RAN J., Facile preparation and enhanced photocatalytic H_2-production activity of $Cu(OH)_2$ cluster modified TiO_2, *Energy & Environmental Science*, **4**(4), 2011, 1364.
13.KUMAR S. G., DEVI L, G., Review on Modified TiO_2 Photocatalysis Under UV/Visible Light: Selected Results and Related Mechanisms on Interfacial Charge Carrier Transfer Dynamics, *The Journal of Physical Chemistry A*, **115**(46), 2011, 13211-13241.
14.DOLIVEIRA J., Al-SAYYED G., PICHAT P., Photodegradation of 2- and 3-chlorophenol in titanium dioxide aqueous suspensions, *Environ.sci.technol*, **24**(7) 1990, 990-996.
15.ZHU JIAXIN, XIONG YUHUA, GUO RUI, Research progress in modification of TiO_2 photocatalyst, *Inorganic Chemicals Industry*, **52**(03), 2020, 23-27.
16.CHEN M. J., LO S. L., LEE Y C., et al. Photocatalytic decomposition of perfluorooctanoic acid by transition-metal modified titanium dioxide, *Journal of Hazardous Materials*, **288**, 2015, 168-175.
17.MARINA, RATOYA, et al. Visible light active photocatalytic C-doped titanium dioxide films deposited via reactive pulsed DC magnetron co-sputtering: Properties and photocatalytic activity, *Vacuum*, 149, 2018, 214-224.

18.LIN C. T., SOPAJAREE K., JITJANESUWAN T., et al. Application of visible light on copper-doped titanium dioxide catalyzing degradation of chlorophenols, *Separation and Purification Technology*, **191**, 2017, 233-243.
19.TIAN W., WU H., SU C., et al. Heterostructure based on silver/silver chloride nanocubes loaded titanium dioxide nanofibers: a high-efficient and recyclable visible light-responsive photocatalyst, *Journal of Photochemistry & Photobiology A Chemistry*, **350**, 2018, 122-129.
20.SHARMA S., UMAR A., SOOD S., et al. Photoluminescent C-dots: An overview on the recent development in the synthesis, physiochemical properties and potential applications, *Journal of Alloys and Compounds*, **748**, 2018, 818-853.
21.KANG QIANG LU, QUAN QUAN, NAN ZHANG, YI JUN XU, Multifarious roles of carbon quantum dots in heterogeneous photocatalysis, *Journal of Energy Chemistry*, **25**(06), 2016, 927-935.
22.LIN C., SONG Y., CAO L., et al. Effective photocatalysis of functional nanocomposites based on carbon and TiO_2 nanoparticles, *Nanoscale*, **5**(11), 2013, 4986-4992.
23.ZHANG H., HUANG H., MING H., et al. Carbon quantum dots/Ag_3PO_4 complex photocatalysts with enhanced photocatalytic activity and stability under visible light, *Journal of Materials Chemistry*, **22**(21):2012, 10501-10506.
24.DENG Y., CHEN M., CHEN G., et al. Visible-Ultraviolet Upconversion Carbon Quantum Dots for Enhancement of the Photocatalytic Activity of Titanium Dioxide, *ACS Omega*, **6**, 2021, 4247-4254.
25.ZHANG B., MAIMAITI H., ZHANG D. D., et al. Preparation of Coal-Based C-Dots/TiO_2 and its Visible-Light Photocatalytic Characteristics for Degradation of Pulping Black Liquor, *Journal of Photochemistry and Photobiology A: Chemistry*, **345**, 2017, 54-62.
26.MAMATJAN YIMIT, GVLMIRA HASAN, 2019, China Patent No. 201911366966.6
27.SHARMA S., MEHTA S K., IBAHDON A. O., et al. Fabrication of novel Carbon Quantum Dots modified Bismuth Oxide (α-Bi_2O_3/C-dots): Material Properties and Catalytic Applications, *Journal of Colloid and Interface Science*, 2018, 533.
28.KAUR A., GUPTA G., IBHADON A. O., et al. A Facile synthesis of silver modified ZnO nanoplates for efficient removal of ofloxacin drug in aqueous phase under solar irradiation, *Journal of Environmental Chemical Engineering*, **6**, 2018, 3621-3630.
29.PING CHEN, FENGLIANG WANG, ZHIFENG CHEN, et al. Study on the photocatalytic mechanism and detoxicity of gemfibrozil by a sunlight-driven TiO_2/carbon dots photocatalyst: The significant roles of reactive oxygen species, *Applied Catalysis B: Environmental*, **204**, 2017, 250-259.
30.ZHENG XIAOYING, HE AOXI, CHEN JIN, et al. Preparation of TiO_2 with microwave heating and investigation of its phase transformation, *Mining & Metallurgy*, **27**(06), 2018, 38-41.
31.YAXIN ZHANG, ZEYU ZHOU, TAN CHEN, et al. Graphene TiO_2 nanocomposites with high photocatalytic activity for the degradation of sodium pentachlorophenol, *Journal of Environmental Sciences*, **26**(10), 2014, 2114-2122.
32.PAN D., JIAO J., LI Z., et al. Efficient Separation of Electron–Hole Pairs in Graphene Quantum Dots by TiO_2 Heterojunctions for Dye Degradation, *Acs Sustainable Chemistry & Engineering*, **3**, 2015, 191-197.
33.YU H., ZHAO Y., ZHOU C., et al. Carbon quantum dots/TiO_2 composites for efficient photocatalytic hydrogen evolution, *Journal of Materials Chemistry A*, **2**(10), 2014, 3344-3351.
34.KUMAR M. S., YASODA K. Y., KUMARESAN D., et al. TiO_2-carbon quantum dots (CQD) nanohybrid: enhanced photocatalytic activity, *Materials Research Express*, **5**(7), 2018, 075502.
35.CHENG L, WANG C, LIU Z. Upconversion nanoparticles and their composite nanostructures for biomedical imaging and cancer therapy, *Nanoscale*, **5**(1), 2012, 23-37.
36.WANG Y, ZHANG H, LIU P, et al. Engineering the band gap of bare titanium dioxide materials for visible-light activity: a theoretical prediction, *Rsc Advances*, **3**(23):2013, 8777-8782.

Manuscript received: 11. 06. 2021